Inorganic Chemistry

Article

pubs.acs.org/IC

Dizinc Cation $[Zn_2]^{2+}$ Trapped In A Homoleptic Metalloid Coordination Environment Stabilized by Dispersion Forces: $[Zn_2(GaCp^*)_6][BAr_4^F]_2$

Kerstin Freitag,[†] Hung Banh,[†] Christian Gemel,[†] Paul Jerabek,[‡] Rüdiger W. Seidel,[†] Gernot Frenking,*[,‡] and Roland A. Fischer*[,‡]

[†]Inorganic Chemistry II—Organometallics and Materials, Ruhr-University Bochum, D-44780 Bochum, Germany

[‡]Department of Chemistry, Philipps University Marburg, D-35032 Marburg, Germany

Supporting Information

ABSTRACT: The synthesis and characterization of the cationic mixed metal Ga/Zn cluster $[Zn_2(GaCp^*)_6]^{2+}$ (**1**) is presented. The reaction of $[Zn_2Cp^*_2]$ with $[Ga_2Cp^*][BAr_4^F]$ leads to the formation of the novel complex being the first example of a $[Zn_2]^{2+}$ core exclusively ligated by metalloid group-13 organyl-ligands. Compound **1** exhibits two different coordination modes: In the solid state, two of the six GaCp* ligands occupy bridging positions, whereas VT ^{1}H NMR indicates the coexistence of a second isomer in solution featuring six terminal GaCp* ligands. Quantum chemical calculations have been carried out to assign the gallium and zinc positions; the bonding situation in **1** is characterized and the importance of dispersion forces is discussed.

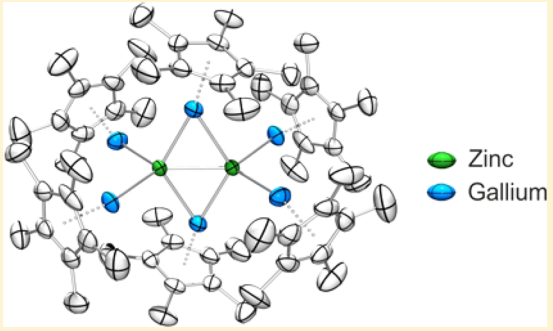

INTRODUCTION

Carmonas discovery of dizincocene, $[Zn_2Cp^*_2]$, the first molecular example for a covalent 2-electron 2-center Zn—Zn interaction, substantially enriched and generally advanced the chemistry of metal—metal bonded low-oxidation state $[M_2R_2]$ compounds (M = Mg, Zn; R = bulky substituents).[1−3] Typical reactivity patterns of $[Zn_2Cp^*_2]$ have been investigated during the past years and are summarized in Scheme 1. From a conceptual and retro-synthetic point of view, the Cp* ligand can be regarded as a protection group for the still unknown, "naked" (i.e., solvated) $[Zn_2]^{2+}$ unit. Selective splitting-off the Cp* group by single-electron oxidation or protolysis may either yield semi or fully "de-protected" dizinc species, stabilized by solvent or other Lewis-base ligands. Examples include the mono cation $[Cp^*Zn{-}Zn(OEt_2)_3]^+$, the dication $[Zn_2(dmap)_6]^{2+}$ (dmap = 4-(dimethylamino)-pyridine) or the triple-decker monocation $[Cp^*_3Zn_4(Et_2O)_2]^+$, which latter structure features two intact Zn—Zn units sharing one central η^3-Cp* ligand.[4,5] Thus, the value of the Cp* group is characteristically different in this chemistry from the other more rigid and not (easily or selectively) removable bulky substituents R, such as $(C_6H_3\text{-}2,6\text{-}(C_6H_3\text{-}2,6\text{-}^iPr_2)_2)$ or DipNacnac $[(DipNCMe)_2CH]$, Dip = 2-6-$C_6H_3{}^iPr_2$), which are also frequently used to stabilize $[M_2]^{2+}$ core units.[3,6] The reactivity of $[Zn_2Cp^*_2]$ toward transition metal (TM) complexes $[L_nTM]$ is also rich and interesting in this respect. Both species, Cp*Zn and/or Cp*ZnZn, can act as one electron ligators as well as selective Cp* transfer reagents. Furthermore, disproportionation of $[Zn_2Cp^*_2]$ yields Cp^*_2Zn and Zn(0), which latter species can be trapped at the TM center: For example, the treatment of $[TM(cod)_2]$ (TM = Ni, Pt) with $[Zn_2Cp^*_2]$ yields $[Cp^*TM(ZnCp^*)_3]$.[7] However, reactions with $[Pd(CH_3)_2(tmeda)]$ (tmeda = *N,N,N′,N′*-tetramethyl-ethane-1,2-diamine) are more delicate. Only traces of $[Cp^*Pd(ZnCp^*)_3]$ are formed besides $[Pd(ZnCp^*)_4(ZnMe)_4]$ and $[Pd(ZnCp^*)_4(ZnMe)_2(Zn\{tmeda\})]$ as the major products.[8] Combined transfer of Cp*Zn and the intact ZnZnCp* unit is possible, too: $[TM(GaCp^*)_a(ZnCp^*)_{4-a}(ZnZnCp^*)_{4-a}]$ (TM = Pd, Pt; a = 0, 2).[9] Related Ga/Zn exchange reactions, using GaCp* transition metal complexes of the general formula $[TM(GaCp^*)_n]$ as starting compounds, yield a series of homoleptic zinc rich complexes $[TM(ZnR)_{2n}]$ (TM = $n \geq 4$; TM = Mo, Ru, Rh, Ni, Pd, Pt; R = Me, Et, Cp*).[10,11] These reactions proceed via combined exchange reactions of R between Ga and Zn coupled to redox processes, involving the reduction of Zn(II) to Zn(I) and the oxidation of Ga(I) giving Ga(III) species, which were identified by *in situ* NMR studies.

The above summarized reactivity patterns of $[Zn_2Cp^*_2]$ and its synthetic equivalence to GaCp* as a source of Zn(I) ligands in transition metal complex and cluster chemistry motivated us to study the coordination chemistry of GaCp* at Zn-centers. In 2007, we reported on the synthesis and structure of the Zn(II)-complex $[Zn(GaCp^*)_4]^{2+}$, which was obtained by protolysis of $ZnMe_2$ with $[H(OEt_2)_2][BAr^F_4]$ in fluorobenzene and *subsequent* addition of Cp*Ga.[12] The complex is isoelectronic to the 18 valence electron nickel congener $[Ni(GaCp^*)_4]$.[13] Interestingly, we have now found that $[Zn_2Cp^*_2]$ is fully inert

Received: October 17, 2014
Published: December 17, 2014

   dx.doi.org/10.1021/ic502532g | *Inorg. Chem.* 2015, 54, 352−358

Scheme 1. Typical Reactivity Patterns of "Carmonas Reagent", $[Zn_2Cp^*_2]$[1,2]

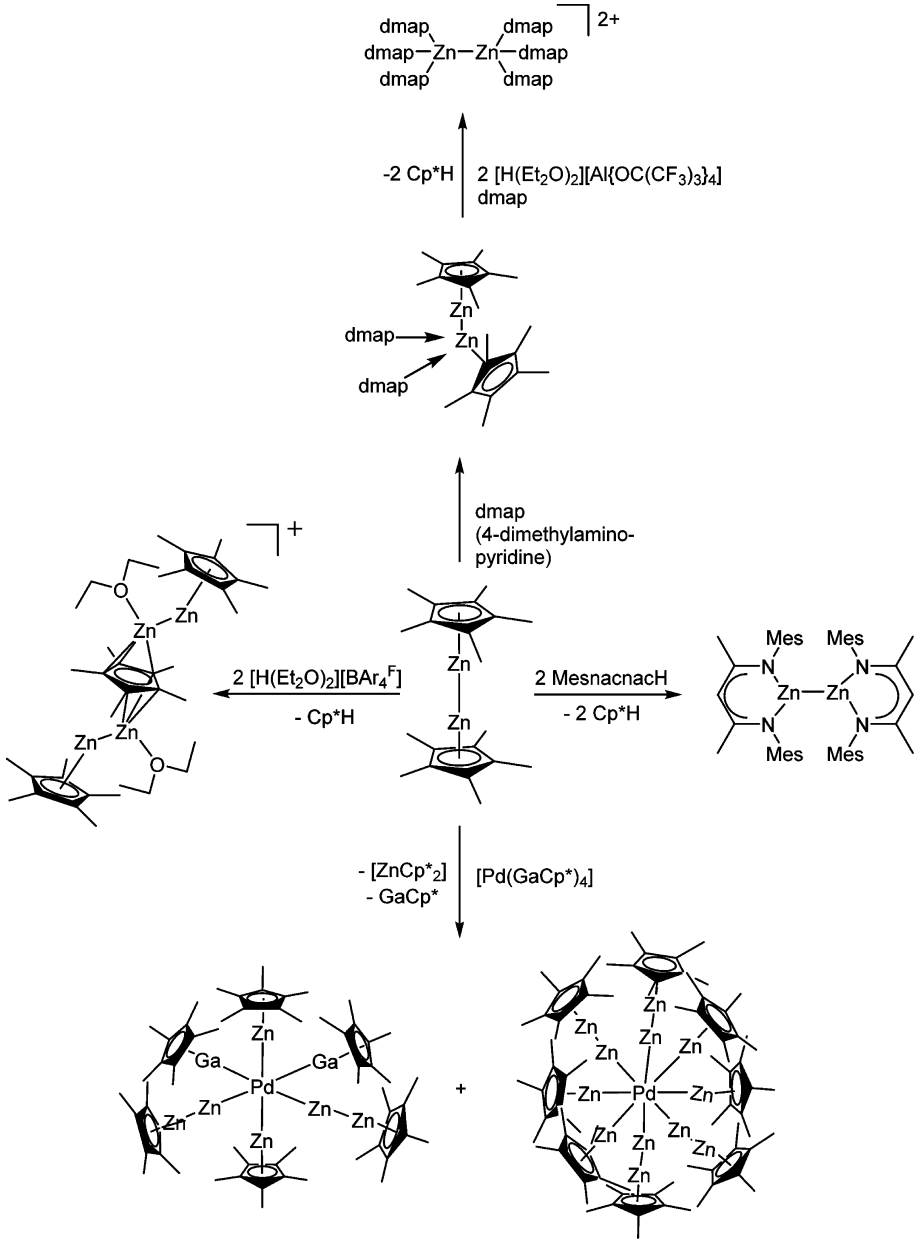

toward GaCp*. There is no indication of any Ga/Zn adduct formation (by in situ NMR) and, moreover, we did not isolate anticipated species of the kind $[Cp^*Zn{-}Zn(\eta^1\text{-}Cp^*)(GaCp^*)_2]$, which are formally equivalent to existing Lewis-base adducts of $[Zn_2Cp^*_2]$ such as $[Cp^*Zn{-}Zn(\eta^1\text{-}Cp^*)(dmap)_2]$.[5] We have neither found any indication of species like $[Cp^*Ga(ZnCp^*)_2]$ or $[Ga(ZnCp^*)_3]$, which are suggested by the isolobal analogy H ↔ ZnCp*. Their molecular structures would feature so far unknown covalent Ga−Zn two center two electron bonds, rather than Ga → Zn donor−acceptor bonds (as it is the case in the complex dication $[Zn(GaCp^*)_4]^{2+}$). Thus, the reactivity motive known from transition metal chemistry, e.g., homolytic cleavage of the Zn−Zn bond and trapping of two Cp*Zn units at an electron deficient center [TM] to yield $[Cp^*Ni(ZnCp^*)_3]$ or $[Pd(ZnCp^*)_4(ZnZnCp^*)_4]$ cannot (directly) be transferred to main group metal centers [M].[7,9] We reasoned that Cp*Ga may be sterically too demanding and electronically too saturated and therefore we decided to use $[Ga_2Cp^*][BAr_4^F]$ as a reaction partner for $[Zn_2Cp^*_2]$. The cation $[Ga_2Cp^*]^+$ can be regarded as a synthetic equivalent of substituent-free, "naked" Ga^+ (i.e., solvated in fluorobenzene).[14] It transfers highly Lewis-acidic and redox-labile Ga^+ to electron rich metal centers. For example, the penta-coordinated Pt(0) complex cation $[GaPt(GaCp^*)_4]^+$ is obtained by treatment of $[Pt(GaCp^*)_4]$ with $[Ga_2Cp^*][BAr_4^F]$.[15] Thus, we expected to yield species such as cationic $[(\mu\text{-}Ga)Zn_2Cp^*_2]^+$ (i.e., Zn−Zn bond bridged by Ga^+) or the neutral $[Ga(ZnCp^*)_3]$ (i.e., the RZn-analogue of GaH_3). In fact $[Ga_2Cp^*][BAr_4^F]$ turned out to be reactive against $[Zn_2Cp^*_2]$ (Scheme 2). However, we isolated the title compound of this Article, $[Zn_2(GaCp^*)_6][BAr_4^F]_2$ ($\mathbf{1}[BAr_4^F]_2$). Its structure features the $[Zn_2]^{2+}$ core unit of Zn(I) wrapped into a homoleptic shell of GaCp* 2-electron donor ligands. Thus, compound **1** is the immediate Zn(I) analogue of the Zn(II) complex $[Zn(GaCp^*)_4]^{2+}$ and the metal-atom ligator analogue of classic donor−acceptor

dx.doi.org/10.1021/ic502532g | Inorg. Chem. 2015, 54, 352−358

Scheme 2. Synthesis of the Hexa-Gallium Coordinated Di-Zinc Title Compound $[Zn_2(GaCp^*)_6][BAr_4^F]_2$ ($\mathbf{1}[BAr_4^F]_2$)

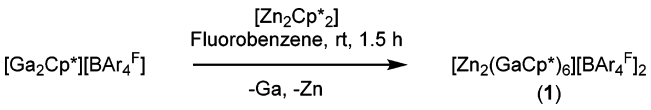

complexes $[Zn_2L_6]^{2+}$ (e.g., L = dmap). In this Article, we describe and discuss the synthesis, compositional analysis and spectroscopic properties, as well as elucidation of the solid state structure and the bonding situation.

EXPERIMENTAL SECTION

Synthesis Techniques and Starting Materials. All manipulations were carried out in an atmosphere of purified argon using standard Schlenk and glovebox techniques. Hexane was dried using an MBraun Solvent Purification System. Fluorobenzene was dried over Al_2O_3. The final H_2O content in all solvents was checked by Karl Fischer titration. $[Ga_2Cp^*][BAr_4^F]$ and $[Zn_2Cp^*_2]$ were prepared according to literature known procedures.[14,16,17] Elemental analysis was performed by the Kolbe Microanalytics Laboratory, Mülheim an der Ruhr, Germany. NMR spectra were recorded on a Bruker DPX-250 spectrometer (^1H, 250.1 MHz; ^{13}C, 62.9 MHz) in CD_2Cl_2 in the range between −90 °C and room temperature. Chemical shifts are given relative to TMS and were referenced to the residual solvent resonances as internal standards. FT-IR spectra were measured on a Bruker Alpha FT-IR spectrometer.

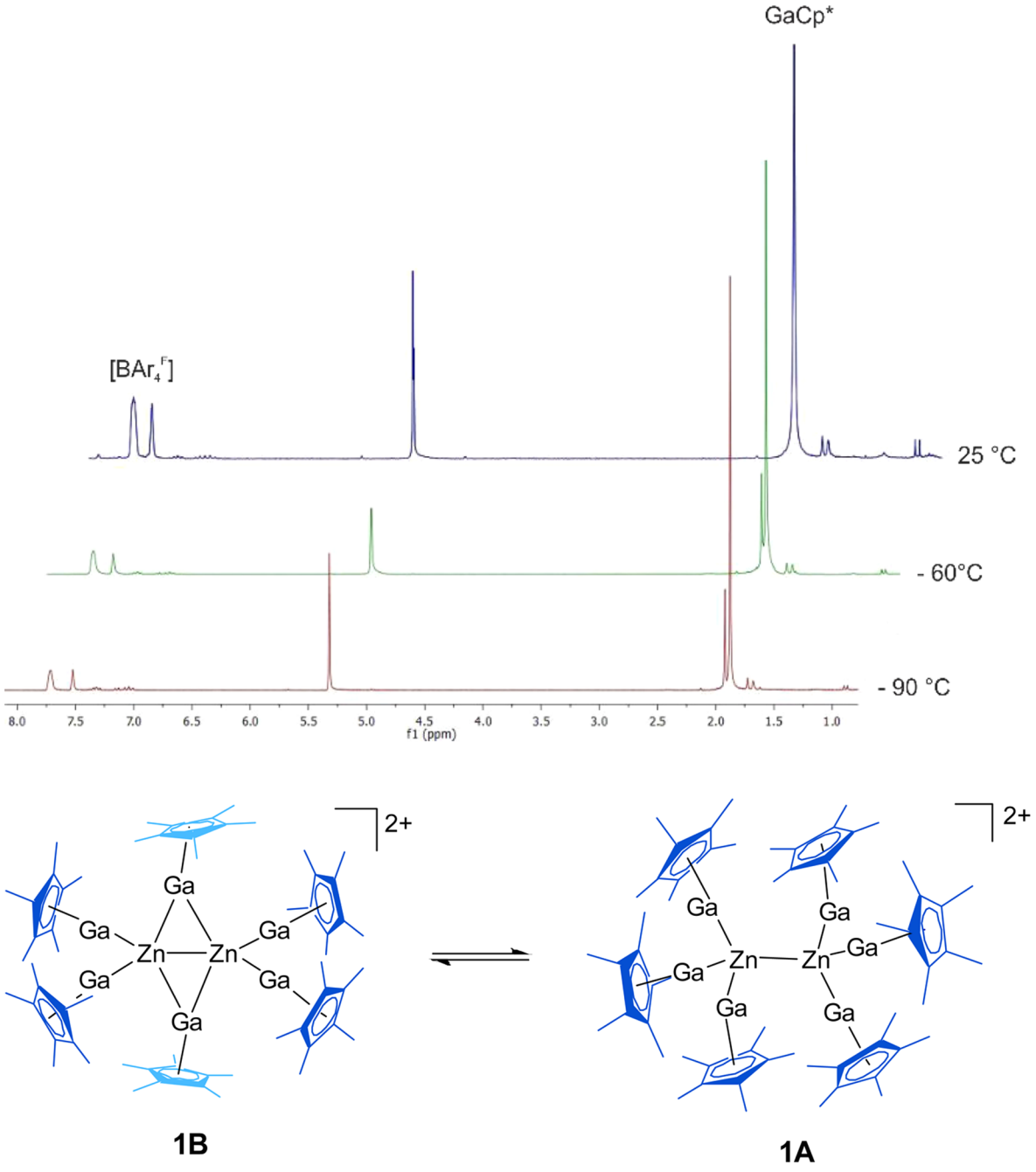

Figure 1. Temperature-dependent ^1H NMR spectroscopy of $\mathbf{1}[BAr_4^F]_2$. Equilibrium of the two coordination isomers **1A** and **1B**.

dx.doi.org/10.1021/ic502532g | Inorg. Chem. 2015, 54, 352−358

*Preparation of $[Zn_2(GaCp^*)_6][BAr_4^F]_2$ (**1**$[BAr_4^F]_2$).* In total, 80 mg of $[Zn_2Cp^*_2]$ (0.199 mmol) and 227 mg of $[Ga_2Cp^*][BAr_4^F]$ (0.199 mmol) were simultaneously dissolved in 5 mL of fluorobenzene at 25 °C. A yellow solution over a metallic-lustrous precipitate was formed immediately. The reaction mixture was stirred for 1.5 h at 25 °C and centrifuged afterward. The obtained yellow solution was filtrated via cannula and stored at −30 °C. Yellow cubic-shaped crystals of **1**$[BAr_4^F]_2 \cdot 4C_6H_5F$ suitable for single crystal X-ray diffraction were obtained after 48 h and were selected from the obtained batch with the aid of a microscope. The remaining amount of crystalline product was separated from the mother liquor by decantation and washed three times with 3 mL of cold *n*-hexane and then dried in dynamic oil pump vacuum. Yield: 161 mg (26% of the theory). The collected precipitate was washed, dried, and analyzed via dispersive X-ray fluorescence (EDX) and turned out to contain the elements Ga and Zn in a molar ratio of 1:23.

*Analytical Data of **1**$[BAr_4^F]_2$.* ^{1}H NMR (298 K, 250.1 MHz, CD_2Cl_2) δ [ppm]: 2.05 (s, 90H, C_5Me_5), 7.56 (s, 16H, BAr_4^F), 7.72 (s, 8H, BAr_4^F). ^{1}H NMR (208 K, 250.1 MHz, CD_2Cl_2) δ [ppm]: 1.88 (s, 150H, C_5Me_5 (terminal)), 1.92 (s, 30H,C_5Me_5 (bridging)), 7.52 (s, 32H, BAr_4^F), 7.72 (s, 16H, BAr_4^F). ^{13}C NMR (298 K, 250.1 MHz, CD_2Cl_2) δ [ppm]: 9.86 (s, C_5Me_5), 116.95 (s, BAr_4^F), 117.97 (C_5Me_5), 124.97 (q, J_{C-F} = 272.1 Hz, CF_3), 129.39 (q, J_{C-F} = 31.6 Hz, BAr_4^F), 135.29 (s, BAr_4^F), 162.18 (q, J_{C-B} = 51.9 Hz, BAr_4^F). ^{19}F NMR (298 K, 250.1 MHz, CD_2Cl_2) δ [ppm]: −62.87. IR (ATR, 298 K) [cm^{-1}]: 2903 (w), 1596 (m), 1446 (w), 1401 (m), 1379 (m), 1341 (s), 1265 (s), 1102 (m), 939 (m), 922 (m), 888 (m), 877 (s), 831 (s), 789 (m), 738 (s), 707 (s), 676 (s), 662 (s), 578 (w), 444 (s), 406 (m)

Elemental and AAS analysis [%] calculated for $C_{148}H_{134}B_2F_{52}Ga_6Zn_2$ (**1**$[BAr_4^F]_2 \cdot 4C_6H_5F$): C 51.21, H 3.89, Zn 3.77, Ga 12.05. Found: C 47.19, H 3.05, Zn 3.57, Ga 10.81. Note: the somewhat large deviation from expected values can probably be attributed to sample deterioration due to moisture and not cooling during sample transfer and handling for elemental analysis.

Single Crystal Structure Determination. The X-ray intensity data for **1**$[BAr_4^F]_2 \cdot 4C_6H_5F$ were collected on an Agilent Technologies SuperNova diffractometer with an Atlas CCD detector, using CuK_α radiation (λ = 1.541 84 Å) from multilayer X-ray optics. The crystals were coated with a perfluoropolyether, picked up with a cryo loop, and immediately mounted in the nitrogen cold gas stream of the diffractometer. The data were processed with CrysAlisPro.[18] An absorption correction based on multiple-scanned reflections was carried out with ABSPACK in CrysAlisPro. The crystal structure was solved by direct methods using SHELXS-97 and refined with SHELXL-2013.[19] Two of the CF_3 groups of the BAr_4^F anion show rotational disorder, and the fluorobenzene solvent molecules were each found disordered over three positions. Disordered parts were modeled with appropriate restraints and constraints on geometry and atomic displacement parameters (ADPs). Anisotropic ADPs were introduced for all non-hydrogen atoms except for the fluorobenzene solvent molecules. Hydrogen atoms were placed at geometrically calculated positions and refined with the appropriate riding model. CCDC 1023640 contains the supplementary crystallographic data for this paper. These data can be obtained free of charge from the Cambridge Crystallographic Data Centre via www.ccdc.cam.ac.uk/data_request/cif.

Computational Methods and Techniques. The geometries of the molecules have been optimized at BP86/def2-TZVPP using the RI approximation with the program Turbomole V6.4.2.[20−26] Stationary points have been characterized by calculating the Hessian matrices. Dispersion interactions were computed with Grimme's D3 correction in conjuction with the Becke−Johnson damping function.[27,28] The EDA calculations were carried out at the BP86 level in conjunction with TZ2P+ Slater functions with and without D3(BJ) correction at the BP86-D3(BJ)/def2-TZVPP optimized geometry using the ADF(2013.01) program.[29,30] For further details see the Supporting Information.

RESULTS AND DISCUSSION

Synthesis and Composition. The reaction of $[Zn_2Cp^*_2]$ with an equimolar amount of $[Ga_2Cp^*][BAr_4^F]$ in fluorobenzene at 25 °C immediately leads to the formation of a yellow solution as well as a metallic-lustrous precipitate of Ga/Zn (Scheme 2). As indicated by EDX spectroscopy, the metal precipitate contains gallium as well as zinc. In situ NMR studies of the filtrated reaction solution revealed a very clean spectrum of only one singlet signal assigned to **1** (Figure 1, see discussion below) and only trace amounts of Cp*H (as the typical impurity observed in this chemistry). Other likely side products, such as Cp^*_2Zn, Cp^*_2 (decamethylfulvalene), free Cp*Ga, or any other Cp*, were not detected. Concentration and storage of the reaction solution at −30 °C gives $[Zn_2(GaCp^*)_6][BAr_4^F]_2 \cdot 4C_6H_5F$ (**1**$[BAr_4^F]_2 \cdot 4C_6H_5F$) as yellow cubic crystals, suitable for single crystal X-ray diffraction. The typical isolated yield (~25−30%) is rather low due to the high solubility of the compound in fluorobenzene. However, as indicated by ^{1}H NMR spectroscopy, the mother liquor does not contain detectable amounts of any other organic or organometallic species. The isolated crystals of **1**$[BAr_4^F]_2 \cdot 4C_6H_5F$ are stable under inert gas atmosphere at −30 °C but decompose within a few hours at room temperature and even more rapidly after redissolving the compound in (various) organic solvents.

The assignment of the Ga/Zn elemental composition of **1** based on single crystal X-ray diffraction is difficult, since gallium and zinc cannot unambiguously be distinguished from each other by routine single crystal X-ray diffraction, owing to very similar scattering power of the two neighboring elements in the periodic table. Unfortunately, the extreme sensitivity to moisture, air, and temperature ruled out shipping the crystals for more sophisticated structural analysis at synchrotron X-ray or neutron sources. Thus, indirect reasoning, taking the results of various analytical methods and computational modeling at the advanced DFT level of theory into account, led to a consistent assignment of the molecular structure of **1**. First, the Zn/Ga metal content was determined by atomic absorption spectroscopy (AAS) after digestion of the very same single crystalline batch from which the specimens were selected for subsequent X-ray analysis. The metal contents measured for compound **1**$[BAr_4^F]_2 \cdot 4C_6H_5F$ (Zn 3.57%, Ga 10.81%) deviate from the calculated values for the expected empirical formula: $C_{148}H_{134}B_2F_{52}Ga_6Zn_2$ (Zn 3.77%, Ga 12.05%). However, the experimental value obtained for the molar Zn/Ga ratio of 2.0:5.7 is essentially consistent with the proposed metal composition of Zn_2Ga_6. The deviation in absolute values is most likely a consequence of the high thermal instability of **1**$[BAr_4^F]_2$ at room temperature (decomposition, loss of solvent C_6H_5F molecules).

^{1}H and ^{13}C NMR Spectroscopy. The room temperature ^{1}H NMR spectrum exhibits a single sharp resonance at δ = 2.05 ppm, indicating the presence of chemically equivalent Cp* groups, besides the expected set of signals assigned to the two BAr_4^F anions and traces of Cp*H. Obviously, there is a fast fluxional process exchanging terminal and bridging Cp* moieties. At lower temperatures, the signal decoalesces, i.e., at −60 °C two broad singlets are observed at δ = 1.92 and 1.88 ppm, however, showing an unexpected integral ratio of 1:5 (Figure 1). The signals become only slightly sharper at −90 °C. However, the expected integral ratio for a static structure with two bridging and four terminal GaCp* ligands is 1:2. A

dx.doi.org/10.1021/ic502532g | Inorg. Chem. 2015, 54, 352−358

reasonable explanation for this deviation of expected/observed integral ratios is the existence of two isomers in solution, one in accordance with the solid state structure with bridging and terminal GaCp* ligands (**1B**), the other one with terminal GaCp* ligands only (**1A**). Two of the expected three signals of this isomer mixture are overlapping, which is a reasonable assumption taking the usually very small shift differences of coordinated GaCp* ligands as well as the fact into account that the signals at −90 °C are still considerably broadened. It should be noted that the spectra at different temperatures are reversible and also reproducible, ruling out partial decomposition during NMR measurement. However, another possible explanation of this temperature dependent behavior would be dissociation of GaCp* in solution and fast association/dissociation equilibria at higher temperatures, the smaller low temperature signal at 1.92 ppm representing free GaCp*. Although this explanation cannot be ruled out completely, the high shift difference of the smaller signal to the signal of GaCp* in neat CD_2Cl_2 (2.04 ppm) would still remain unexplained. The ^{13}C NMR spectrum measured at room temperature shows the expected resonances for the BAr_4^F anion and one set of resonances assigned for the chemically equivalent Cp* moieties, although gradual decomposition of **1** is indicated by the detection of resonances for free Cp*H and the appearance of a metal precipitate in the NMR tube.

Mechanistic Considerations. Although we cannot provide hard experimental data on mechanistic studies at this point we wish to provide a short qualitative reasoning on the observed formation of **1**. Obviously, the reaction generally proceeds along the reactivity patterns and concepts outlined in the Introduction. It is reasonable to assume an initial Ga^+ transfer from $[Ga_2Cp^*]^+$ to $[Zn_2Cp^*_2]$ possibly by electrophilic attack to the electron Zn−Zn bond. Note that transition metal clusters with substituent-free Ga^+ in an edge-bridging position, i.e., a structural (μ^2-Ga)M_2 moiety are known.[31,32] Then, Cp* transfer from Zn to Ga may take place and a GaCp* species may be formed and trapped as a coordinated ligand. In a way, Ga^+ plays the role of H^+, which is known to "deprotect" the $[Zn_2]^{2+}$ unit by splitting off Cp*H. However, parallel redox processes take place which cause the deposition of Ga(0) and Zn(0). Note, both reaction partners, $[Ga_2Cp^*]^+$ and $[Zn_2Cp^*_2]$, are prone to disproportionation too. Soluble organometallic Ga(III) and Zn(II) byproducts (impurities) can be ruled out by in situ NMR; however, solvated Ga^{3+} and Zn^{2+} cations may be present and escaped our trails to elucidate the spectrum of possible side products. It is notable that $[ZnCp^*_2]$ and $[Ga_2Cp^*]^+$ do not react under formation of a new Ga/Zn mixed metal species but only show coalescence of the signals indicating fast Cp* transfer reactions. An obvious and more straightforward way to obtain higher yields of $\mathbf{1}[BAr_4^F]_2$ would be a classic ligand substitution reaction and treating substitution labile $[Zn_2L_6]^{2+}$ with excess of GaCp*. However, access to such species is limited by now and we are currently investigating access to substitution labile solvated $[Zn_2(solv)]^{2+}$.

Single Crystal Structure Determination. $\mathbf{1}[BAr^F]_2 \cdot 4C_6H_5F$ crystallizes in the triclinic space group $P\bar{1}$ with one formula unit per unit cell. Figure 2 shows the molecular structure of the cation **1**, which is located on an inversion center in the crystal. The assignment of the Zn and Ga sites in the structure refinement is consistent with the elemental analysis and the NMR data. As pointed out already in the previous section, an unambiguous distinction between Ga/Zn is

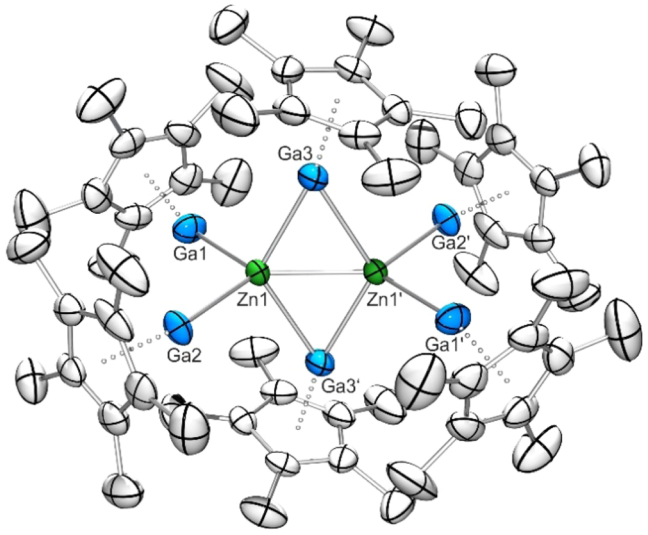

Figure 2. Molecular structure of the dication $[Zn_2(\mu\text{-}GaCp^*)_2(GaCp^*)_4]^{2+}$ (**1**) in the crystal as determined by single crystal X-ray diffraction. Displacement ellipsoids are drawn at the 50% probability level; hydrogen atoms are omitted for clarity. Symmetry-related atoms (1−*x*, 1−*y*, 1−*z*) are primed. Selected interatomic distances (Å) and angles (deg): Zn1−Zn1′ 2.411(1), Zn1−Ga1 2.456(1), Zn1−Ga2 2.459(1), Zn1−Ga3 2.585(1), Zn1−Ga3′ 2.511(1), Ga−$Cp^*_{centroid}$ diameter = 1.909, Ga1−Zn1−Ga2 103.55(2), Ga1−Zn1−Ga3 108.19(2), Ga2−Zn1−Ga3 108.85(2), Ga3−Zn1−Ga3′ 123.53(2), Zn1−Ga3−Zn1′ 56.47(2), Zn1−Ga1−$Cp^*_{centroid}$ 162.46, Zn1−Ga2−$Cp^*_{centroid}$ 170.10, Zn1−Ga3−$Cp^*_{centroid}$ 135.64, Zn1−Ga3′−$Cp^*_{centroid}$ 166.64.

difficult based on the available routine X-ray diffraction data. Swapping gallium and zinc positions in **1** in the structure refinement as well as assuming disordered Ga/Zn positions for all eight metal positions did not lead to significant enhancement of essential parameters like temperature factors, dimensions of the thermal ellipsoids, or the *R*-values. Therefore, we should note that a different distribution of Zn and Ga over the eight metal atom positions cannot rigorously be ruled out on the basis of the X-ray data. However, the computational analysis at the advanced DFT level of theory presented in the next section provides clear evidence for the assignment. The Zn−Zn distance in the core of **1** (2.412(1) Å) is elongated in comparison to the parent compound $[Zn_2Cp^*_2]$ (2.305(3) Å) but only slightly elongated compared to other $[Zn_2R_2]$ compounds like $[Zn_2Tp^{Me2}{}_2]$ Tp = tris(3,5-dimethylpyrazolyl)-hydridoborate).[1,6,33] The Ga−Zn bonds for the terminal GaCp* ligands are virtually the same (2.456(1) and 2.459(1) Å) and well comparable with literature known Ga−Zn bonds.[12,34] As expected, the appropriate distances for the bridging ligands are elongated (2.511(1) and 2.585(1) Å). The Ga-$Cp^*_{centroid}$ distances (diameter = 1.909 Å) are quite short and indicate rather electrophilic gallium centers, which is in accordance with the doubly positively charged complex and the coordinative binding to Zn^+ centers. This effect is even stronger observed in $[Zn(GaCp^*)_4]^{2+}$ were the values for the Ga-$Cp^*_{centroid}$ bonds are 1.850 and 1.861 Å.[12] Both zinc atoms are tetrahedrally coordinated by four gallium atoms each. Two of the Ga−Zn−Ga bond angles (Ga1−Zn1−Ga3 103.55(2)°, Ga2−Zn1−Ga3 108.19(2)°) slightly deviate from the perfect tetrahedral angle of 109.5°. The Ga1−Zn1−Ga2 angle (103.55(2)°) diverges more strongly, which can most probably be attributed to the steric influence of the zinc−zinc bond. As a

dx.doi.org/10.1021/ic502532g | *Inorg. Chem.* 2015, 54, 352−358

consequence, the Ga3−Zn−Ga3′ angle is enlarged (123.53(2)°) while the Zn1−Ga3−Zn1′ angle only measures 56.47(2)°. Resulting from the tetrahedral arrangement, the Ga3−Zn1 (2.585(1) Å and Ga3−Zn1′ (2.511(1) Å) bond length differ. The Zn1−Ga−Cp*$_{centroid}$ angles deviate from linearity of the terminal GaCp* ligands (162.46 and 170.10°), presumably owing to steric effects and the bridging GaCp* groups (135.64 and 166.64°).

Structural Modeling and Bonding Situation. Quantum chemical calculations using density functional theory (DFT) at the BP86/TZVPP level of theory together with the D3(BJ) correction by Grimme have been carried out for the dication **1**. We used the X-ray structure of **1** as a starting point for the geometry optimization of the modeled structure **M1A** (Figure 3). During the calculation, the two bridging GaCp* ligands moved into terminal positions and gave the structure which is shown in Figure 3 as a minimum on the potential energy surface. Several attempts were made to locate an isomer with bridging GaCp* ligands similar to the observed isomer **1B** in the crystal structure. All calculations gave a geometry with only terminal ligands which resembles the structure of isomer **1A** (Scheme 2) which is assumed to be also present in solution (NMR spectroscopy) (*vide supra*). We think that the doubly bridged isomer **1B** becomes stabilized by packing together with the two counterions $[BAr_4^F]^-$ in the solid state during the crystallization.

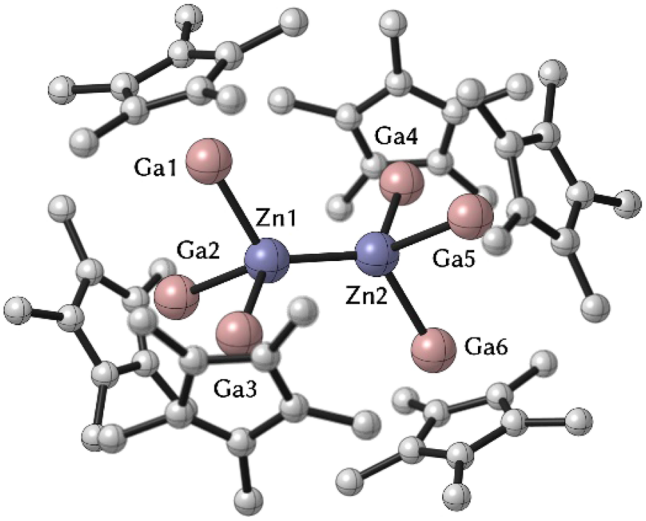

Figure 3. Calculated structure of **M1A**. The bond lengths refer to the values at BP86-D3(BJ)/TZVPP; the data without dispersion corrections at BP86/TZVPP are given in brackets. The experimental values of the bridged isomer are shown in parentheses. All data are in Å. Hydrogen atoms are omitted for a better view. Bond lengths: Zn1−Zn2 2.361 [2.461] (2.411), Ga1−Zn1 2.498 [2.601] (2.459), Ga2−Zn1 2.456 [2.598] (2.456), Ga3−Zn1 2.517 [2.603] (2.585), Ga4−Zn2 2.515 [2.603] (2.585), Ga5−Zn2 2.461 [2.598] (2.456), Ga6−Zn2 2.487 [2.601] (2.459).

It is interesting to note that the calculated Ga−Zn distances of the optimized structure **M1A** with terminal GaCp* ligands are quite similar to the experimental values for the bridged isomer **1B** which are also shown in Figure 1. The geometry optimization of **M1** which was carried out without any symmetry constraints gave three different Ga−Zn bond lengths for the Zn(GaCp*)$_3$ moieties between 2.456 and 2.517 Å and 2.461 and 2.515 Å (Figure 3). The X-ray structure analysis of the bridged isomer has two short bonds of 2.456 and 2.459 Å and one long bond of 2.585 Å at each Zn(GaCp*)$_3$ fragment. The data in Figure 3 suggest that the dispersion forces have a significant influence on the calculated Ga−Zn bond lengths of **1MA** which become much shorter at BP86-D3(BJ)/TZVPP. The impact of dispersion interactions comes also to the fore when the nature of the Zn−Zn bond is investigated with an energy decomposition analysis (EDA). Table 1 shows the results of the EDA calculations for the interactions between two $[Zn(GaCp^*)_3]^+$ fragments in the electronic doublet state at the at BP86-D3(BJ)/TZVPP optimized geometry. The calculations show that the intrinsic interaction ΔE_{int} between the positively charged fragments $[Zn(GaCp^*)_3]^+$ with frozen geometries are attractive but the attraction comes mainly from the dispersion interaction. The intrinsic Zn−Zn bonding amounts only to ΔE_{int} = −3.6 kcal/mol while the total attraction is ΔE_{int} = −51.5 kcal/mol. A similar situation has recently been reported by Grimme and Schreiner for substituted hexaphenylethanes where bulky substituents at the phenyl groups stabilize the molecule and yield a "C−C bonded" molecule Ar_3C-CAr_3 which is held together only by dispersion forces.[35] The breakdown of the interaction energy ΔE_{int} $[(GaCp^*)_3Zn-Zn(GaCp^*)_3]^{2+}$ into Pauli repulsion ΔE_{Pauli}, electrostatic interaction ΔE_{elstat}, orbital (covalent) bonding ΔE_{orb}, and dispersion interaction ΔE_{disp} shows that one-half of the attraction comes from ΔE_{orb} (51%) while one-quarter each comes from ΔE_{elstat} (25%) and ΔE_{disp} (24%).

Table 1. EDA Results in kcal/mol for the Interactions between Two $[Zn(GaCp^*)_3]^+$ Fragments in the Electronic Doublet State in the Calculated Structure of 1 with and without Dispersion Correction[a]

	BP86-D3(BJ)/TZ2P+	BP86/TZ2P+
ΔE_{int}	−51.5	−3.6
ΔE_{Pauli}	145.4	145.4
ΔE_{elstat}	−49.2 (25.0%)	−49.2 (33.0%)
ΔE_{orb}	−99.8 (50.7%)	−99.8 (67.0%)
ΔE_{disp}	−48.0 (24.4%)	

[a]The fragments $[Zn(GaCp^*)_3]^+$ were calculated in the electronic doublet state.

CONCLUSION

In connection with our studies on the coordination chemistry of low valent organo group-12 and group-13 compounds at transition metals centers, we presented herein a novel and purely Zn/Ga "cluster" species. The right choice of gallium and zinc precursors leads to the formation of the organometallic, mixed metal dication $[Zn_2(GaCp^*)_6]^{2+}$. It is another rare example of the coordination chemistry of Zn(I) and the first case of a homoleptic all-metal atom ligated $[Zn_2]^{2+}$ core. Interestingly, the cluster cation **1** features two coordination isomers **1A** and **1B** in solution. While the solid state structure exhibits two GaCp* ligands in bridging and four ligands in terminal positions (**1B**), low temperature ^{1}H NMR spectroscopy indicates the existence of a second isomer in solution with six terminal GaCp* ligands (**1A**). Isomers **1A** and **1B** show a fast equilibrium in solution. Quantum chemical calculations give only one energy minimum structure for **1** where the GaCp* ligands prefer the terminal positions (**1MA**). The bonding analysis of the Zn−Zn interaction suggests that the molecule **1MA** is held together mainly by dispersion forces.

dx.doi.org/10.1021/ic502532g | *Inorg. Chem.* 2015, 54, 352−358

The doubly bridged isomer **1MB**, which corresponds to the structure of **1** found by X-ray crystallography of the solvated salt $\mathbf{1}[BAr_4^F]_2\ C_6H_5F_4$, is not a minimum structure in the calculations. Obviously the exclusively observed isomer **1B** in the solid state is favored by packing effects induced by the counteranion and the solvate molecules (i.e., dispersion forces), factors for which the theoretical modeling and analysis of **1** cannot account for at this point.

■ ASSOCIATED CONTENT

Supporting Information

Crystallographic data in CIF format; NMR and IR spectra (Figures S2−S7); as well as further details regarding quantumchemical calculations. This material is available free of charge via the Internet at http://pubs.acs.org.

■ AUTHOR INFORMATION

Corresponding Authors

*E-mail: frenking@chemie.uni-marburg.de.
*E-mail: roland.fischer@rub.de. Fax: (+49) 234-32-12174.

Notes

The authors declare no competing financial interest.

■ ACKNOWLEDGMENTS

This work was supported by the DFG (Grant Fi-502/23-2). K.F. and H.B are grateful for a scholarship of the German Chemical Industry Fund (https://www.vci.de/fonds). The dissertation project of K.F. is further supported by the RUB Research School (http://www.research.school.rub.de)

■ REFERENCES

(1) Resa, I.; Carmona, E.; Gutierrez-Puebla, E.; Monge, A. *Science* **2004**, *306*, 1136−1138.
(2) Li, T.; Schulz, S.; Roesky, P. W. *Chem. Soc. Rev.* **2012**, *41*, 3759−3771.
(3) Jones, C. *Coord. Chem. Rev.* **2010**, *254*, 1273−1289.
(4) Freitag, K.; Banh, H.; Ganesamoorthy, C.; Gemel, C.; Seidel, R. W.; Fischer, R. A. *Dalton Trans.* **2013**, *42*, 10540−10544.
(5) Schulz, S.; Schuchmann, D.; Krossing, I.; Himmel, D.; Blaeser, D.; Boese, R. *Angew. Chem., Int. Ed.* **2009**, *48*, 5748−5751.
(6) Zhu, Z.; Brynda, M.; Wright, R. J.; Fischer, R. C.; Merrill, W. A.; Rivard, E.; Wolf, R.; Fettinger, J. C.; Olmstead, M. M.; Power, P. P. *J. Am. Chem. Soc.* **2007**, *129*, 10847−10857.
(7) Bollermann, T.; Freitag, K.; Gemel, C.; Seidel, R. W.; Fischer, R. A. *Organometallics* **2011**, *30*, 4123−4127.
(8) Bollermann, T.; Freitag, K.; Gemel, C.; Molon, M.; Seidel, R. W.; von Hopffgarten, M.; Jerabek, P.; Frenking, G.; Fischer, R. A. *Inorg. Chem.* **2011**, *50*, 10486−10492.
(9) Bollermann, T.; Freitag, K.; Gemel, C.; Seidel, R. W.; von Hopffgarten, M.; Frenking, G.; Fischer, R. A. *Angew. Chem., Int. Ed.* **2011**, *50*, 772−776.
(10) Cadenbach, T.; Bollermann, T.; Gemel, C.; Fernandez, I.; von Hopffgarten, M.; Frenking, G.; Fischer, R. A. *Angew. Chem., Int. Ed.* **2008**, *47*, 9150−9154.
(11) Cadenbach, T.; Bollermann, T.; Gemel, C.; Tombul, M.; Fernandez, I.; van Hopffgarten, M.; Frenking, G.; Fischer, R. A. *J. Am. Chem. Soc.* **2009**, *131*, 16063−16077.
(12) Kempter, A.; Gemel, C.; Cadenbach, T.; Fischer, R. A. *Inorg. Chem.* **2007**, *46*, 9481−9487.
(13) Jutzi, P.; Neumann, B.; Schebaum, L. O.; Stammler, A.; Stammler, H.-G. *Organometallics* **1999**, *18*, 4462−4464.
(14) Buchin, B.; Gemel, C.; Cadenbach, T.; Schmid, R.; Fischer, R. A. *Angew. Chem., Int. Ed.* **2006**, *45*, 1074−1076.
(15) Buchin, B.; Gemel, C.; Cadenbach, T.; Fernandez, I.; Frenking, G.; Fischer, R. A. *Angew. Chem., Int. Ed.* **2006**, *45*, 5207−5210.
(16) del Rio, D.; Galindo, A.; Resa, I.; Carmona, E. *Angew. Chem., Int. Ed.* **2005**, *44*, 1244−1247.
(17) Grirrane, A.; Resa, I.; Rodriguez, A.; Carmona, E.; Alvarez, E.; Gutierrez-Puebla, E.; Monge, A.; Galindo, A.; Del Rio, D.; Andersen, R. A. *J. Am. Chem. Soc.* **2007**, *129*, 693−703.
(18) *CrysAlisPro Software System*, version 1.171.36.20; Agilent Technologies UK Ltd.: Oxford, U.K., 2012.
(19) Sheldrick, G. M. *Acta Crystallogr.* **2008**, *A64*, 112−122.
(20) Becke, A. D. *Phys. Rev. A: Gen. Phys.* **1988**, *38*, 3098−100.
(21) Perdew, J. P. *Phys. Rev. B* **1986**, *33*, 8822−8824.
(22) Ahlrichs, R.; Baer, M.; Haeser, M.; Horn, H.; Koelmel, C. *Chem. Phys. Lett.* **1989**, *162*, 165−169.
(23) Ahlrichs, R. *Phys. Chem. Chem. Phys.* **2004**, *6*, 5119−5121.
(24) Eichkorn, K.; Treutler, O.; Oehm, H.; Haeser, M.; Ahlrichs, R. *Chem. Phys. Lett.* **1995**, *242*, 652−660.
(25) Eichkorn, K.; Weigend, F.; Treutler, O.; Ahlrichs, R. *Theor. Chem. Acc.* **1997**, *97*, 119−124.
(26) Weigend, F. *Phys. Chem. Chem. Phys.* **2006**, *8*, 1057−1065.
(27) Grimme, S. *J. Comput. Chem.* **2006**, *27*, 1787−1799.
(28) Grimme, S.; Antony, J.; Ehrlich, S.; Krieg, H. *J. Chem. Phys.* **2010**, *132*, 154104/1−154104/19.
(29) Snijders, J. G.; Vernooijs, P.; Baerends, E. J. *At. Data Nucl. Data Tables* **1981**, *26*, 483−509.
(30) SCM, Theoretical Chemistry. *ADF*, 2013.01; Vrije Universiteit: Amsterdam, The Netherlands; http://www.scm.com.
(31) Halbherr, M.; Bollermann, T.; Gemel, C.; Fischer, R. A. *Angew. Chem., Int. Ed.* **2011**, *49*, 1878−1881.
(32) Cadenbach, T.; Gemel, C.; Schmid, R.; Halbherr, M.; Yusenko, K.; Cokoja, M.; Fischer, R. A. *Angew. Chem., Int. Ed.* **2009**, *48*, 3872−3876.
(33) Gondzik, S.; Blaeser, D.; Woelper, C.; Schulz, S. *Chem.—Eur. J.* **2010**, *16*, 13599−13602.
(34) Jones, C.; Rose, R. P.; Stasch, A. *Dalton Trans.* **2007**, 2997−2999.
(35) Grimme, S.; Schreiner, P. R. *Angew. Chem., Int. Ed.* **2011**, *123*, 12849−12853.